

Analyze of the star formation modeling algorithm in SPH code

Peter Berczik

Main Astronomical Observatory of Ukrainian National Academy of Sciences,
UA-03680, Golsiiv, Kiev-127, Ukraine, e-mail: berczik@mao.kiev.ua

November 17, 2000

Abstract. The chemical and photometric evolution of star forming disk galaxies is investigated. Numerical simulations of the complex gasdynamical flows are based on our own coding of the *Chemical-Dynamical Smoothed Particle Hydrodynamical* (CD-SPH) approach, which incorporates the effects of star formation. As a first application, the model is used to describe the chemical and photometric evolution of a disk galaxy like the Milky Way.

Keywords: star formation, chemical and photometric evolution, SPH code

1. Introduction

Galaxy formation is a highly complex subject requiring many different approaches of investigation. Recent advances in computer technology and numerical methods have allowed detailed modeling of baryonic matter dynamics in a universe dominated by collisionless dark matter and, therefore, the detailed gravitational and hydrodynamical description of galaxy formation and evolution. The most sophisticated models include radiative processes, star formation and supernova feedback, e.g. (Katz, 1992; Steinmetz & Muller, 1994; Friedli & Benz, 1995).

The results of numerical simulations are fundamentally affected by the star formation algorithm incorporated into modeling techniques. Yet star formation and related processes are still not well understood on either small or large spatial scales. Therefore the star formation algorithm by which gas is converted into stars can only be based on simple theoretical assumptions or on empirical observations of nearby galaxies.

Among the numerous methods developed for modeling complex three dimensional hydrodynamical phenomena, Smoothed Particle Hydrodynamics (SPH) is one of the most popular (Monaghan, 1992). Its Lagrangian nature allows easy combination with fast N -body algorithms, making possible the simultaneous description of complex gas-stellar dynamical systems (Friedli & Benz, 1995). As an example of such a combination, TREE-SPH code (Hemquist & Katz, 1989; Navarro & White, 1993) was successfully applied to the detailed



© 2024 Kluwer Academic Publishers. Printed in the Netherlands.

modeling of disk galaxy mergers (Mihos & Hernquist, 1996) and of galaxy formation and evolution (Katz, 1992). A second good example is an GRAPE – SPH code (Steinmetz & Müller, 1994; Steinmetz & Müller, 1995) which was successfully used to model the evolution of disk galaxy structure and kinematics.

2. The model

The hydrodynamical simulations are based on our own coding of the *Chemical-Smoothed Particle Hydrodynamics* (CD – SPH) approach, including feedback through star formation (SF). The dynamics of the "star" component is treated in the framework of a standard N – body approach. Thus, the galaxy consists of "gas" and "star" particles. For a detailed description of the CD – SPH code (the star formation algorithm, the SN II, SN Ia and PN production, the chemical enrichment and the initial conditions) the reader is referred to (Berczik & Kravchuk, 1996; Berczik, 1999; Berczik, 2000). Here we briefly describe the basic features of our algorithm.

2.1. Star formation algorithm

It is well known that SF regions are associated with giant molecular complexes, especially with regions that are approaching dynamical instability. The overall picture of star formation seems to be understood, but the detailed physics of star formation and accompanying processes, on either small or large scales, remains sketchy (Larson, 1969; Silk, 1987).

All the above stated as well as computer constraint cause the using of simplified numerical algorithms of description of conversion of the gaseous material into stars, which are based on simple theoretical assumptions and/or on results of observations of nearby galaxies.

We modify the "standard" SPH SF algorithm (Katz, 1992; Steinmetz & Müller, 1994; Steinmetz & Müller, 1995), taking into account the presence of chaotic motion in the gaseous environment and the time lag between the initial development of suitable conditions for SF, and SF itself.

Inside a "gas" particle, the SF can start if the absolute value of the "gas" particles gravitational energy exceeds the sum of its thermal energy and its energy of chaotic motions:

$$|E_i^{gr}| \geq E_i^{th} + E_i^{ch} : \quad (1)$$

Gravitational and thermal energies and the energy of random motions for the "gas" particle i in model simulation are defined as:

$$\begin{aligned} E_i^{\text{gr}} &= \frac{3}{5} G \frac{m_i^2}{h_i}; \\ E_i^{\text{th}} &= \frac{3}{2} m_i c_i^2; \\ E_i^{\text{ch}} &= \frac{1}{2} m_i v_i^2; \end{aligned} \quad (2)$$

where $c_i = \sqrt{\frac{P}{\rho_i}}$ is the isothermal sound speed of particle i . We set $\gamma = 1.3$ and define the random or "turbulent" square velocities near particle i as:

$$v_i^2 = \frac{X_B}{m_j} \sum_{j=1}^N (v_j - v_c)^2 = \frac{X_B}{m_j} \sum_{j=1}^N v_j^2; \quad (3)$$

where:

$$v_c = \frac{X_B}{m_j} \sum_{j=1}^N v_j; \quad (4)$$

For practical reasons, it is useful to define a critical temperature for SF onset in particle i as:

$$T_i^{\text{crit}} = \frac{8}{3} \left(\frac{G}{h_i} m_i v_i^2 \right); \quad (5)$$

Then, if the temperature of the "gas" particle i , drops below the critical one, SF can proceed.

$$T_i < T_i^{\text{crit}}; \quad (6)$$

The chosen "gas" particle produces stars only if the above condition holds over the time interval exceeding its free-fall time:

$$t_{\text{ff}} = \frac{1}{\sqrt{G \rho_i}}; \quad (7)$$

We also check that the "gas" particles remain cool, i.e. $t_{\text{cool}} < t_{\text{ff}}$. We rewrite these conditions following (Navarro & White, 1993):

$$t_i > t_{\text{crit}}; \quad (8)$$

We set the value of $t_{\text{crit}} = 0.03 \text{ cm}^{-3}$.

When the collapsing particle i is defined, we create the new "star" particle with mass m^{star} and update the "gas" particle m_i using these simple equations:

$$\begin{aligned} m^{\text{star}} &= m_i; \\ m_i &= (1 - \epsilon) m_i; \end{aligned} \quad (9)$$

In the Galaxy, on the scale of giant molecular clouds, the typical values for SF efficiency are in the range 0.01–0.4 (Duerr et al., 1982; Wilking & Lada, 1983).

We did not fix this value but rather also derived from the "energetic" condition:

$$= 1 - \frac{E_i^{\text{th}} + E_i^{\text{ch}}}{\sum_j E_j^{\text{gr}}}. \quad (10)$$

At the moment of birth, the positions and velocities of new "star" particles are set equal to those of parent "gas" particles. Thereafter these "star" particles interact with other "gas" and "star" or "dark matter" particles only by gravity.

2.2. Thermal SN II feedback

For the thermal budget of the ISM, SN II play the main role. Following to (Katz, 1992; Friedli & Benz, 1995), we assume that the energy from the explosion is converted totally to thermal energy. The total energy released by SN II explosions (10^{44} J per SN II) within "star" particles is calculated at each time step and distributed uniformly between the surrounding "gas" particles (Raiteri et al., 1996).

2.3. Chemical enrichment of gas

In our SF scheme, every new "star" particle represents a separate, gravitationally bound, star formation macro region (like a globular cluster). The "star" particle has its own time of birth t_{begSF} which is set equal to the moment the particle is formed. After the formation, these particles return the chemically enriched gas into surrounding "gas" particles due to SN II, SN Ia and PN events.

We concentrate our treatment only on the production of ^{16}O and ^{56}Fe , yet attempt to describe the full galactic time evolution of these elements, from the beginning up to present time (i.e. $t_{\text{evol}} = 15.0$ Gyr).

2.4. Photometric evolution of star component

The code also includes the photometric evolution of each "star" particle, based on the idea of the Single Stellar Population (SSP) (Bressan et al., 1994; Tantaló et al., 1996).

At each time-step, absolute magnitudes: $M_U, M_B, M_V, M_R, M_I, M_K, M_M$ and M_{bol} are defined separately for each "star" particle. The SSP integrated colours (UBVR_IKM) are taken from Tantaló et al. (1996). The spectro-photometric evolution of the overall ensemble of "star" particles forms the Spectral Energy Distribution (SED) of the galaxy.

We do not model the energy distribution in spectral lines nor the scattered light by dust. However according to Tantaló et al. (1996) our approximation is reasonable, especially in the UVB spectral band.

2.5. Initial conditions

As the initial model (relevant for CDM -scenario) we took a constant density homogeneous gaseous triaxial configuration ($M_{\text{gas}} = 10^{11} M_{\odot}$) within the rigid Plummer type dark matter halo ($M_{\text{halo}} = 10^{12} M_{\odot}$). We set the scale length of dark matter halo: $b_{\text{halo}} = 25$ kpc. These values of M_{halo} and b_{halo} are typical for dark matter halo in disk galaxies (Navarro et al., 1996; Navarro et al., 1997; Burkert, 1995). We set $A = 100$ kpc, $B = 75$ kpc and $C = 50$ kpc for semiaxes of system. Such triaxial configurations are reported in cosmological simulations of the dark matter halo formation (Eisenstein & Loeb, 1995; Frenk et al., 1988; Warren et al., 1992).

The gas was assumed to be involved in the Hubble flow ($H_0 = 65$ km/s/Mpc) and the solid-body rotation around z -axis. The spin parameter in our numerical simulations is 0.08 , defined in Peebles (1969) as:

$$q = \frac{j L_0}{G (M_{\text{gas}} + M_{\text{halo}})^{5/2}}; \quad (11)$$

L_0 is the total initial angular momentum and E_0^{gr} is the total initial gravitational energy of a protogalaxy. It is to be noted that for a system in which angular momentum is acquired through the tidal torque of the surrounding matter, the standard spin parameter does not exceed

0.11 (Steinmetz & Bartelmann, 1995). Moreover, its typical values range between $0.07^{+0.04}_{-0.05}$, e.g. 0.02 to 0.11 .

3. Results and discussion

Our SPH calculations were carried out for the three different number of "gas" particles $N_{\text{gas}} = 2109; 4109; 11513$. As a "base" model we consider the case with $N_{\text{gas}} = 2109$. For this case we calculate the full evolution of galactic system (i.e. $t_{\text{evol}} = 15.0$ Gyr). According to Navarro & White (1993) and Raiteri et al. (1996), such a number seem adequate for a qualitatively correct description of the system behaviour. Even this small number of "gas" particles produces $N_{\text{star}} = 31631$ "star" particles at the end of the calculation. The other two cases: $N_{\text{gas}} = 4109$ and 11513 we need for the more extensive study of our SF scheme. In the case of $N_{\text{gas}} = 4109$ we calculate the evolution up to

$t_{\text{evol}} = 5.0$ Gyr and in the case $N_{\text{gas}} = 11513$ up to $t_{\text{evol}} = 2.5$ Gyr. In all this two cases within these time scale the total number of particles access the $N_{\text{max}} = 65535$ and after this we, stop any SF activity.

The more extended discussion of the dynamical and chemical data can be found in the papers Berczik (1999) and Berczik (2000). Here we mainly concentrate our attention to the extensive check of our SF scheme and the photometric behaviour of our "base" galaxy model.

In Figure 1 we present the column density distribution –(a) and the rotational velocity distribution – (b) for our "base" galaxy model at the last time step. The total density distribution ($\rho_{\text{tot}} = \rho_{\text{gas}} + \rho_{\text{star}}$) is well approximated by an exponential disk with radial scale length 3.5 kpc. The rotational velocity (V_{rot}) distribution also well coincides with the data for our own galaxy (Vallee, 1994).

In Figure 2a we present the time evolution of "star" particles number N_{star} . In Figure 2b we present the time evolution of the total mass inside "star" particles M_{star} . The number of "star" particle is very different in all three cases, but the total mass inside the "star" component is very similar. Some differences are found only after the SF artificially stops in the models with high "gas" particle numbers. After stop of SF the mass inside "star" component is reduced, according to returning the mass from "star" to surrounding "gas" particles due to SN II, SN Ia and PN events.

The star formation history (SFH – dM_{star}/dt) for all three models is presented in Figure 3. In this figure we clearly see that the SFH practically does not depend on the "gas" or "star" particle number. The star formation efficiency (SFE – %) in each act of SF is presented in the Figure 4. The averaged SFE is about 10%. However we have a wide spread from some percent up to the 50% at the late stage of evolution. In all three models we have a similar SFE trend.

In Figure 5 and Figure 6 we present the chemical evolution of our models. All three models have a very similar chemical history and metallicity distribution.

The total photometric (in UBVK spectral band) and color ($U-B$), ($B-V$), ($V-K$) evolution of our "base" model is presented in the Figure 7a and Figure 7b. In case of our own Milky Way galaxy at the present day we have a value for ($B-V$) 0.8 (van der Kruit, 1986), what is close to our value for model galaxy (0.7).

The color vs. color evolution of the model galaxy presented in Figure 8.

4. Conclusion

The presented model describes well the time evolution of the basic dynamical, chemical and photometric parameters of a disk galaxy similar to the Milky Way. The metallicity, luminosity and colors obtained are typical for such disk galaxies. During the calculations we made an extended test of the proposed new SF criteria. We find that the obtained results with different "gas" and "star" particle numbers are not only qualitatively but also quantitatively similar.

Acknowledgements

The work was supported by the German Science Foundation (DFG) under grants No. 436 UKR 18/2/99, 436 UKR 17/11/99 and partially supported by NATO grant NIG 974675.

Special thanks for hospitality to the Astronomisches Rechen-Institut (ARI) Heidelberg, where part of this work has been done.

It is a pleasure to thank Christian Theis for comments on an earlier version of this paper.

References

- Berczik P. & Kravchuk S.G., 1996, *Ap&SS*, 245, 27
 Berczik P., 1999, *A & A*, 348, 371
 Berczik P., 2000, *Ap&SS*, 271, 103
 Bressan A., Chiosi C. & Fagotto F., 1994, *ApJS*, 94, 63
 Burkert A., 1995, *ApJ*, 447, L25
 Duerr R., Imhof C.L. & Lada C.J., 1982, *ApJ*, 261, 135
 Eisenstein D.J. & Loeb A., 1995, *ApJ*, 439, 520
 Frenk C.S., White S.D.M., Davis M. & Efsthathiou G., 1988, *ApJ*, 327, 507
 Friedli D. & Benz W., 1995, *A & A*, 301, 649
 Hemquist L. & Katz N., 1989, *ApJS*, 70, 419
 Katz N., 1992, *ApJ*, 391, 502
 Larson R.B., 1969, *MNRAS*, 145, 405
 Mihos J.C. & Hemquist L., 1996, *ApJ*, 464, 641
 Monaghan J.J., 1992, *ARA & A*, 30, 543
 Navarro J.F. & White S.D.M., 1993, *MNRAS*, 265, 271
 Navarro J.F., Frenk C.S. & White S.D.M., 1996, *ApJ*, 462, 563
 Navarro J.F., Frenk C.S. & White S.D.M., 1997, *ApJ*, 490, 493
 Peebles P.J.E., 1969, *A & A*, 155, 393
 Raiteri C.M., Villata M. & Navarro J.F., 1996, *A & A*, 315, 105
 Silk J., 1987, in *IAU Symp. No. 115 "Star Forming Regions"*, Eds. Peimbert M. & Jugaku J., Reidel, Dordrecht, p. 557
 Steinmetz M. & Bartelmann M., 1995, *MNRAS*, 272, 570
 Steinmetz M. & Müller E., 1994, *A & A*, 281, L97

- Steinmetz M. & Müller E., 1995, *MNRAS*, 276, 549
Tantaló R., Chiosi C., Bressan A. & Fagotto F., 1996, *A & A*, 311, 361
Vallee J., 1994, *ApJ*, 437, 179
van der Kruit P., 1986, *A & A*, 157, 230
Warren M. S., Quinn P. J., Salmon J. K. & Zurek W. H., 1992, *ApJ*, 399, 405
Wilking B. A. & Lada C. J., 1983, *ApJ*, 274, 698

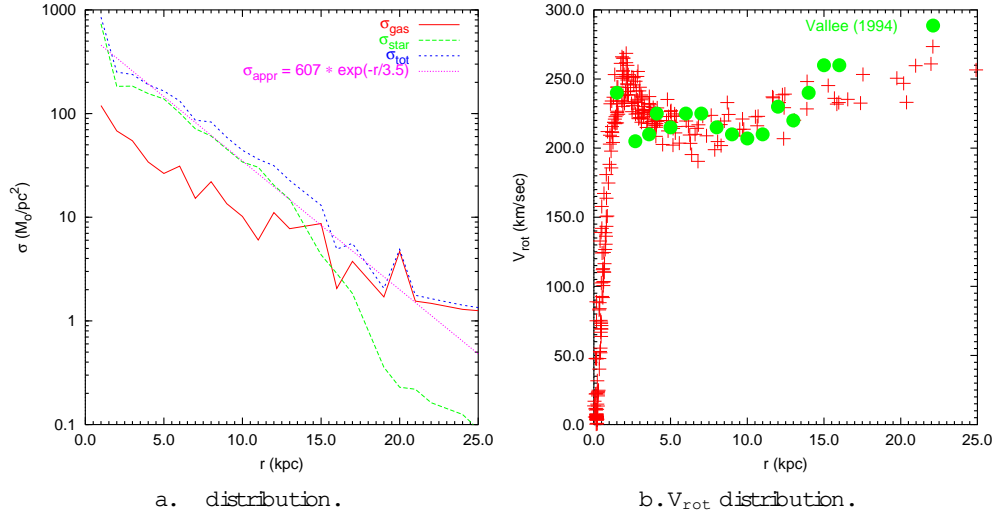


Figure 1. Column density & rotational velocity distribution in the final step for the "basic" model.

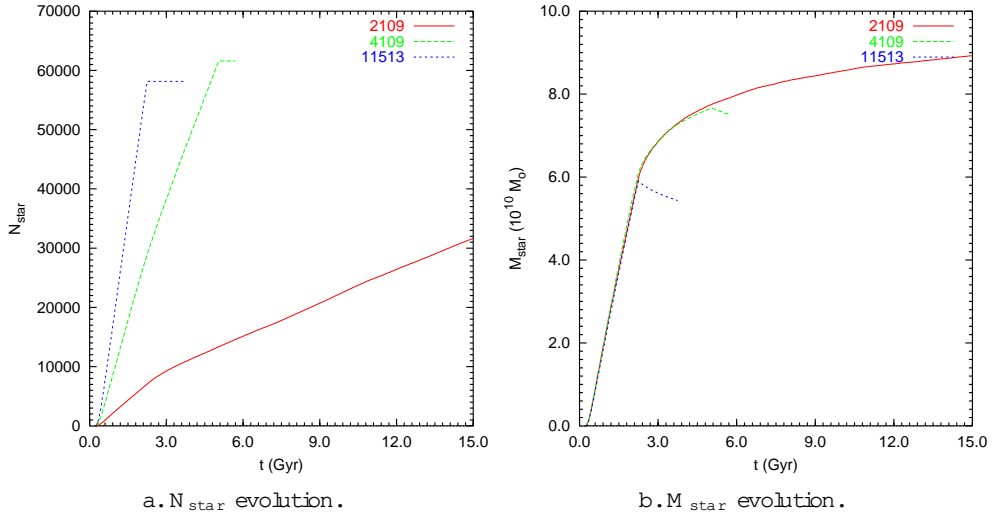


Figure 2. N_{star} & M_{star} evolution of the model galaxy with different "gas" particle number.

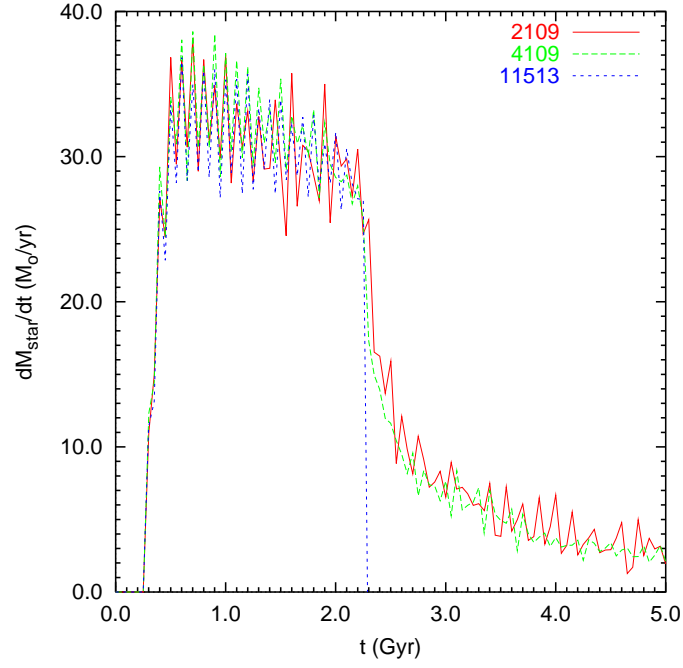


Figure 3. dM_{star}/dt evolution of the model galaxy with different "gas" particle number.

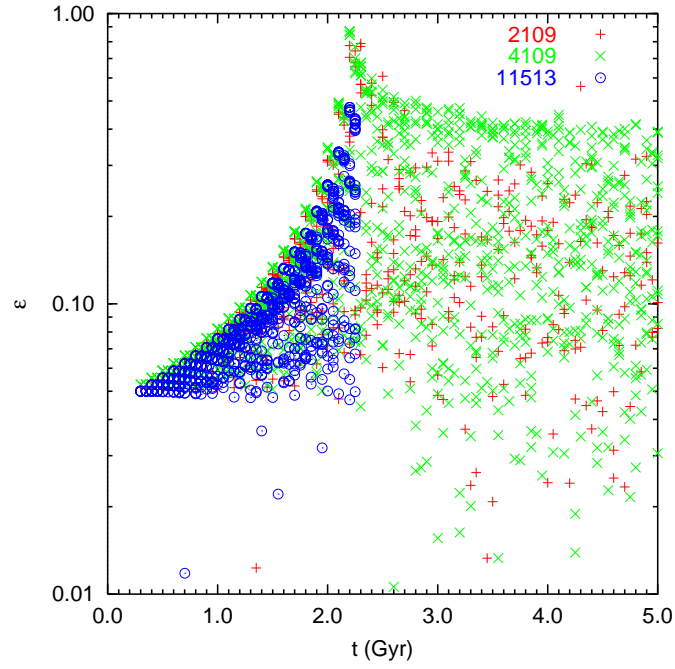


Figure 4. evolution of the model galaxy with different "gas" particle number.

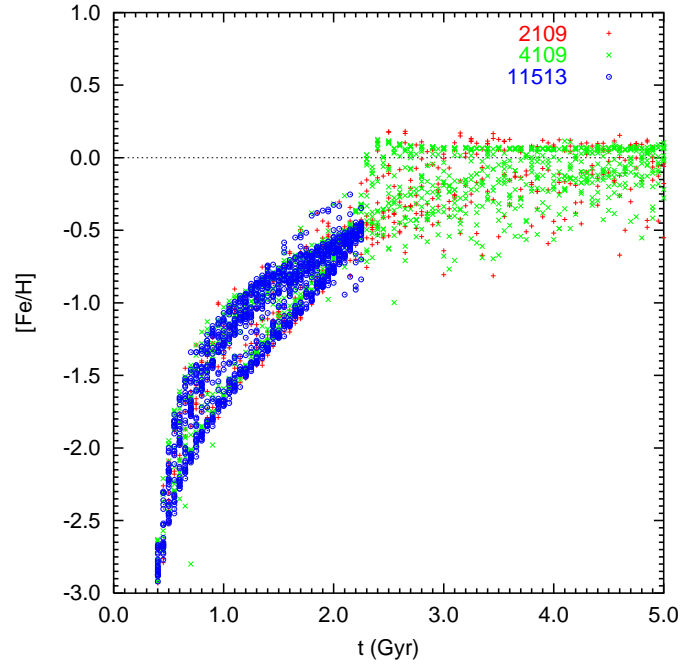


Figure 5. $[\text{Fe}/\text{H}]$ evolution of the model galaxy with different "gas" particle number.

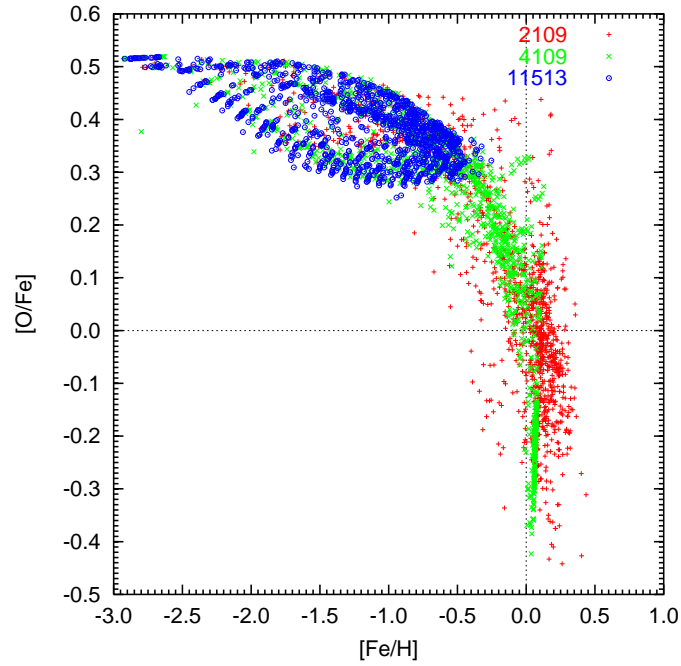


Figure 6. $[\text{O}/\text{Fe}]$ vs. $[\text{Fe}/\text{H}]$ of the model galaxy with different "gas" particle number.

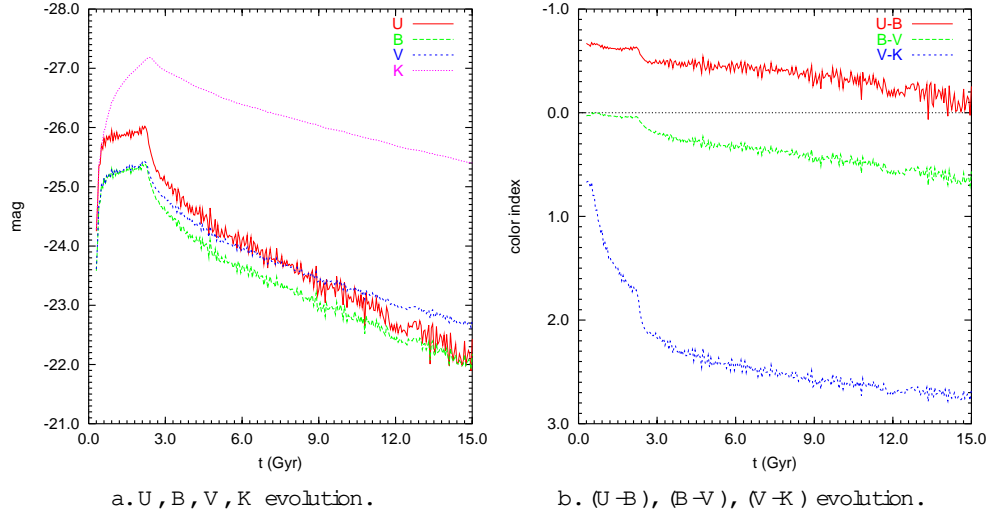


Figure 7. Photometric & color evolution of the galaxy for the "basic" model.

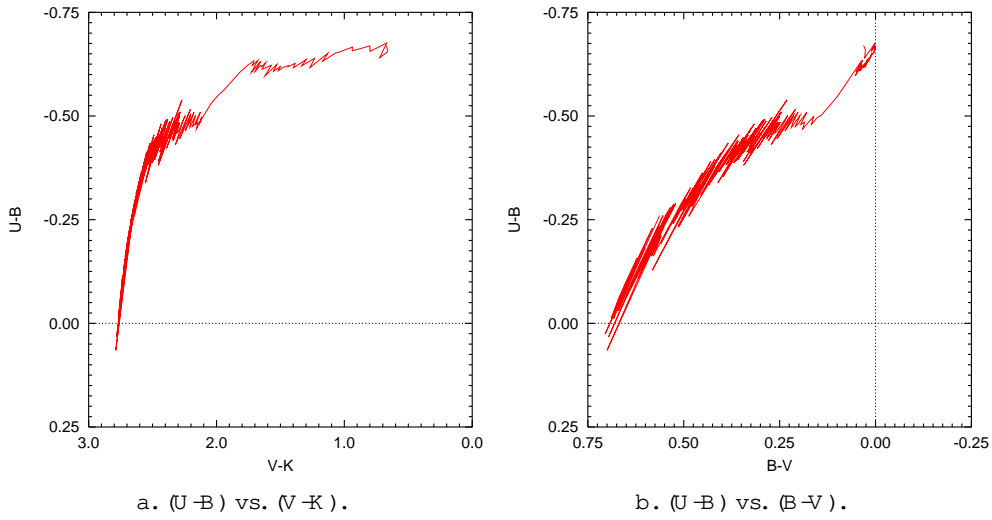


Figure 8. Color vs. color evolution of the galaxy for the "basic" model.